Optimization of Alkali-Treated Banana Pseudo-Stem Fiber/PBAT/PLA Bio-Composite for Packaging Application using Response Surface Methodology

Pei Pei,[a,*] Rui Zou,[a] Chengming Zhang,[b] Menghui Yu,[c] Sandra Chang,[b] Jia Tan,[a] Jiaxin Li,[a] Xuehua Li,[a] and Shizhong Li [b]

The objective of this research was to prepare an optimized bio-composite for packaging based on alkali-treated banana pseudo-stem fiber (BPSF), PBAT, and PLA using response surface methodology (RSM). The effects of three factors, *i.e*., alkali-treated BPSF (0.8 to 2.4 g), PBAT (0.75 to 2.25 g), and PLA (1.6 to 3.2 g) on two dependent variables, *i.e*., bending strength and tensile strength of bio-composite, were investigated. Box-Behnken design (BBD) provided the combination for an optimum composite, which was 1.15 g of alkali-treated BPSF, 2.09 g of PBAT, and 2.66 g of PLA, respectively. The bending strength and tensile strength for alkali-treated BPSF/PBAT/PLA composite were 32.62 MPa and 30.91 MPa, which was 20.50% and 16.51% higher than native BPSF/PBAT/PLA composite. The bio-composite prepared using the optimized results was further characterized by Fourier transform infrared spectroscopy (FTIR), thermogravimetry, scanning electron microscopy (SEM), mechanical testing, contact angles, and water absorption tests. Analyses showed that alkali-treatment could improve the adhesion and compatibility of BPSF in the polymer matrix. These outcomes were associated with the use of treated-BPSF for better mechanical strength and lower hygroscopicity. This result demonstrated that alkali-treated agricultural residue and degradable polymer could be used to prepare composite materials for green packaging application.

DOI: 10.15376/biores.18.1.39-59

Keywords: Alkali-treated banana pseudo-stem fiber (BPSF); PBAT; PLA; Composites for packaging; Response surface methodology

Contact information: a: Department of Information Science and Engineering, Changsha Normal University, Changsha 410000, PR China; b: Institute of Nuclear and New Energy Technology, Tsinghua University, Tsinghua Garden, Beijing 100084, PR China; c: School of Light Industry Science and Engineering, TUST, Tianjin University of Science and Technology, Tianjin 300000, PR China;
** Corresponding author: crispei@163.com*

INTRODUCTION

With the gradual shortage of petroleum resources caused by excessive development and the white pollution problem brought by the widespread use of plastic products, many researchers have begun to look for new materials that can replace traditional petroleum-based materials, as well as protect the environment (Feng *et al*. 2020; Ramle *et al.* 2020; Dixit *et al*. 2021; Gao *et al.* 2021; Rajeshkumar *et al.* 2021; Khosravani and Reinicke 2022). The global plastic production continuously increased from 1.5 million tons in 1950 and is expected to reach 670 million tons by 2035 (Bajracharya *et al*. 2016; Dixit and Yadav 2019). The urgent need to minimize plastic wastes has encouraged the development of

degradable materials as replacements for traditional synthetic polymers (Mansor 2018; El and Vaudreuil 2021; Ribeiro *et al.* 2022). Biodegradable material is a promising substitute in the area of resource circulation development for it could be eventually degraded into H_2O and CO_2 (Gao *et al.* 2021). At the present, China is actively promoting the development of new biodegradable materials.

Different combinations of synthetic polymers are used to produce sustainable composites for packaging applications. Abundantly available biomass and macromolecule polymers (polyethylene, polypropylene, polyvinyl chloride) have been used to synthesize high mechanically stable composites (Razaka *et al.* 2019; Dixit and Yadav 2020; Inseemeesak *et al.* 2022). Lignocellulosic materials such as rice straw, corn straw, sorghum straw, soybean straw, sisal, and hemp are usually used as a substitute in polymer matrix (Xu *et al*. 2019; Feng *et al*. 2020; Zhu *et al*. 2020). Due to the poor compatibility and strong stiffness of lignocellulosic material, native biomass is not very compatible with polymer materials (Bartos *et al*. 2021; Dixit *et al*. 2021). Pretreatment (acid, alkali, oxidants, salts and solvent) of lignocellulosic material before the preparation of composite materials is necessary (Dixit *et al*. 2021). Pretreatment can be used to refine biomass for polymer blending and increase the suitability with polymer matrix (Dixit *et al*. 2021). Pretreated biomass blended with the polymer exhibits a remarkable higher mechanical strength compared to native biomass-based composite (Zegaoui *et al.* 2018; Manral and Bajpai 2021). Among the pretreatment methods, alkali treatment is a promising approach for lignocellulosic materials for use in industrial application.

Banana pseudo-stem (BPS) is an important byproduct of banana. The annual production of BPS is 120 to 165 t per hectare (Pei *et al.* 2014). BPS is an agricultural waste that is available in large quantities, low in price, and biodegradable (Shimizu *et al.* 2018; Neher *et al*. 2020). BPS can be utilized in different fields, such as paper making, rope making, and production of bags and biofuels (Alarcón and Marzocchi 2015; Othman *et al.* 2020; Pan *et al.* 2020). Generally, cellulose, hemicellulose and lignin are found in banana pseudo-stem fiber (BPSF). The utilization of higher cellulosic content of BPSF to substitute for conventionally materials is promising for composite preparation (Khan *et al.* 2013; Ponni *et al.* 2020). The relatively high tensile index and tensile resistance of BPS fiber indicate that these wastes can be used as promising filling materials for reinforcing polymer composites (Alarcón and Marzocchi 2015; Neher *et al*. 2020). Moreover, the influence of chemical treatment on the properties of BPSF/coir hybrid fiber reinforced maleic anhydride grafted polypropylene (MAPP)/low-density polyethylene (LDPE) composites has been examined for food packaging applications (Khan *et al.* 2013). The tensile strength, flexural strength, and impact strength of treated BPSF/MAPP/LDPE blended composites have been reported as 44 MPa, 50 MPa, and 12.5 J/m^2, respectively, which was 15 to 20% higher than untreated samples (Khan *et al.* 2013). Pretreated BPS fiber exhibits better mechanical properties than the untreated ones (Khan *et al.* 2013; Dixit and Yadav 2020). The wide availability of banana pseudo stem makes them a potential source of raw material for processing and production of packaging materials.

Polylactic acid (PLA) is a promising polymer material (Murariu and Dubois 2016; Rajeshkumar *et al.* 2021). It is environmentally friendly, biodegradable, non-toxic, suitable for processing, and harmless to humans (Rajeshkumar *et al.* 2021; Inseemeesak *et al.* 2022). Because the impact strength of PLA is poor, biodegradable poly-butylene adipate-co-terephthalate (PBAT) has been mixed with PLA to improve the toughness and heat resistance of composites (Aliotta *et al*. 2020; Correa-Pacheco *et al.* 2020; Feng *et al*. 2020; Malinowski *et al*. 2020; Gao *et al.* 2021).

Response surface methodology (RSM) is widely used to provide the optimized conditions by analyzing the effects of different independent variables (Albooyeh *et al.* 2022). Many authors have claimed the suitability of using the Box-Behnken design (BBD) of RSM to optimize the independent variables in their research article (Kandar and Akil 2016; Tharazi *et al.* 2017). RSM-BBD is the choice to optimize the process parameters according to our application as well as replace the conventional time-consuming methods (Tharazi *et al.* 2017; Cai *et al.* 2022).

Currently, BPSF is used as the filling material for non-biodegradable polymer (polyvinyl chloride, polypropylene, low-density polyethylene, *etc*.) to produce composite materials (Alarcón and Marzocchi 2015). No relevant research has been reported on the preparation of composites from BPSF, PBAT, and PLA with a goal of producing biodegradable materials. In this paper, alkali-treated BPSF was blended with PBAT and PLA to produce bio-composites for packaging. Different composites designed by RSM-BBD and varying in mass of alkali-treated BPSF, PBAT, and PLA were synthesized. The aim of this paper was to determine the optimum mass of alkali-treated BPSF, PBAT, and PLA for bio-composite with remarkable bending strength and tensile strength. Various techniques were used to characterize the optimized results, including Fourier transform infrared spectroscopy (FTIR), thermogravimetry, scanning electron microscopy (SEM), mechanical tests, contact angles, and water absorption.

EXPERIMENTAL

Materials

Banana pseudo-stem was collected from Hainan Province, China. BPSF was oven-dried at 80 °C for 12 h and sieved through a 100-mesh size.

Alkali treatment of banana pseudo-stem fiber: BPSF (size 100 mesh) was treated with 10 w/v % NaOH aqueous solution at 25 °C for 3 days. Alkali treated BPSF was filtered and washed to neutrality. The desirable biomass residue was oven-dried at 80 °C for 12 h.

Polylactic acid (PLA), size 100 mesh, was procured from ShunJie Plastic Technology Co., LTD, Dongguan, Guangdong Province, China. Poly butylene adipate-co-terephthalate (PBAT), size 100 mesh, was procured from Kexinda Polymer Materials Co., LTD, Shanghai, China. Anhydrous ethanol (95%, liquid) was procured from Sinopharm Chemical Reagent Co. LTD, Shanghai, China. Silane coupling agent (KH-550, liquid) was procured from Shanyi Plastic Chemical Co. LTD, Dongguan, Guangdong Province, China.

Experimental Design and Optimization for Alkali-Treated BPSF/PBAT/PLA Based Bio−Composite

RSM was used to determine the favorable condition for the synthesis of alkali-treated BPSF/PBAT/PLA based bio-composite for packaging application. The proportion of raw materials (three variables: alkali treated BPSF, PBAT, and PLA) was optimized by Box-Behnken design (BBD). Responses (bending strength and tensile strength) obtained from experiments were used to optimize the independent variables. The range and levels of variables were selected based on the results of single-factor tests. The BBD quadratic model of variables in the form of coded and actual values is listed in Table 1.

Table 1. Actual Values and the Corresponding Encoding Levels of Box-Behnken Design

Variable	Range and Levels		
	-1	0	1
x_1- Alkali-treated BPSF (g)	0.8	1.6	2.4
x_2- PBAT (g)	0.75	1.5	2.25
x_3- PLA (g)	1.6	2.4	3.2

This design was represented by a second-order polynomial regression model, as follows,

$$Y = \beta_0 + \sum_{i=1}^{k} \beta_i x_i + \sum_{i=1}^{k} \beta_{ii} x_i^2 + \sum_{1 \le i \le j}^{k} \beta_{ij} x_i x_j + \varepsilon \quad (1)$$

where Y represent the responses (bending strength and tensile strength). The variables x_i, β_0, β_i, β_{ii}, β_{ij}, and ε are the process factors, offset coefficient, linear coefficients, quadratic coefficients, interaction coefficients, and residuals associated with the experiments, respectively. The regression analysis of the experimental data was performed by Design-Expert software (version 8.06) to estimate the response surface and determine the coefficients of the regression equation.

Synthesis of Alkali-Treated BPSF/PBAT/PLA Based Bio−Composite

Alkali-treated BPSF (size 100 mesh) was modified with 5 wt.% silane ethanol solution and dried in an oven at 80 °C. Alkali-treated BPSF, PBAT (size 100 mesh), and PLA (size 100 mesh) were mixed in a ratio recommended by RSM software. The specific composition of composites is shown in Table 2. These materials were evenly mixed for 20 min by a mixer. The uniformly mixed materials were filled into a mold and hot pressed at 170 °C and 8 MPa for 20 min. The preparation process is shown in Fig. 1.

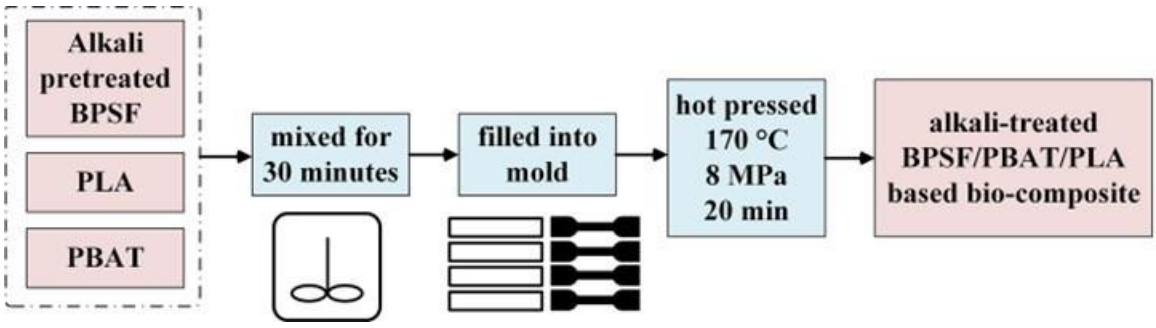

Fig. 1. Synthesis process of alkali-treated BPSF/PBAT/PLA based bio−composite

Analytical Methods

Composition and pH test of BPSF

The composition of cellulose, hemicellulose, and lignin for BPSF before and after alkali treatment were measured using the NREL method (Sluiter *et al*. 2008). The pH of BPSF during alkali treatment was measured by pH meter (Mettler TOLEDO 6219, Mettler Toledo International Co., Ltd. Switzerland).

Mechanical properties of alkali-treated BPSF/PBAT/PLA based bio-composite

The bending strength and tensile strength of bio-composite were tested by universal testing machine (KRWDW-100E, Jinan Kerui Testing Machine Manufacturing Co. LTD, Shandong, China) according to GB/T 9341-2008 and GB/T 1040.2-2022, respectively. Figure 2 shows the dimension of samples prepared for the test of bending strength (80 mm length×10 mm width×4 mm thickness) and tensile strength (dog bone sample, 75 mm length×12 mm width×2 mm thickness). The impact strength of bio-composite was tested by impact testing machine (Digital display impact testing machine ST-5.5D, Xiamen Ester Instrument Co., LTD, Fujian, China) according to GB/T 1043.1-2008 (80 mm length × 10 mm width × 4 mm thickness). Experiments were replicated 3 times to obtain the average value.

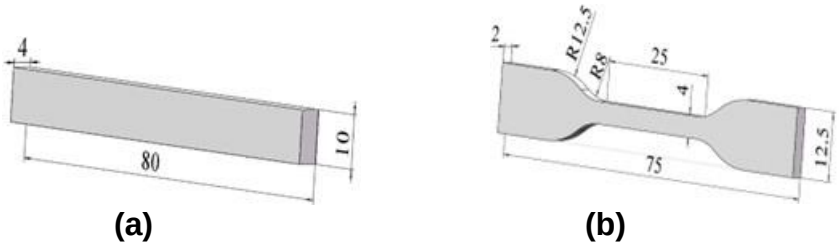

Fig. 2. The dimension of samples prepared for the test of bending strength and tensile strength (a: bending strength; b: tensile strength)

FTIR

The samples were dried at 80 °C for 6 to 8 h. Fourier transform infrared spectrometer (Thermo Scientific Nicolet iS50, Thermo Fisher Scientific, USA) was used to evaluate the infrared spectrum of samples over a wavenumber range from 500 to 4000 cm^{-1}, with a resolution of 4 cm^{-1} and 32 scans. FTIR test was conducted according to Correa-Pacheco *et al.* (2020).

Thermogravimetry

The thermogravimetric curve (TG) of composites was determined using a chip analyzer (Thermogravimetric analyzer TGA 8000, PerkinElmer, Inc, USA). The mass of samples was 10 mg. The heating rate was 10°C /min. The rate of purge gas and protective gas (N_2) was 20 mL/min. The temperature range was 30 to 600 °C. The thermal stability of the bio-composite was measured according to the ASTM E1131 standard test method.

SEM analysis

The surface morphology of PBAT/PLA, native BPSF/PBAT/PLA, and alkali-treated BPSF/ PBAT/PLA based composites were analyzed by using SEM analysis (Field emission scanning electron microscope SU5000, Hitachi High Technology Co, Japan). The surface of samples was treated by spraying gold with an ion sputtering instrument (Aliotta *et al*. 2020; Correa-Pacheco *et al.* 2020)

Contact angle test

A drop shape analyzer (JY-PHa Contact Angle tester, China) was used to evaluate the contact angles of PBAT/PLA, native BPSF/PBAT/PLA, and alkali-treated BPSF/ PBAT/PLA based composites at room temperature. This test was done 5 times, and the average value of the contact angle was calculated to signify the water-resistant property of the composite (Dixit *et al*. 2021).

Water absorption test

The water absorption of PBAT/PLA, native BPSF/PBAT/PLA, and alkali-treated BPSF/ PBAT/PLA based composites was examined referring to ASTM D570 (Ramle *et al.* 2020; Inseemeesak *et al.* 2022). Water absorption test was conducted for 24 hours. Based on the weight change, water absorption was calculated using the following equation,

$$\text{water absorption } (\%) = \frac{m - m_0}{m_0} \times 100 \quad (2)$$

where m_0 and m represent the initial weight and the final weight of sample, respectively.

RESULTS AND DISCUSSION

Effect of Alkali Treatment on Fiber Composition and pH Value of BPSF

The effects of alkali treatment on the content of cellulose, hemicellulose, and lignin for BPSF were investigated. The composition analyses for native and alkali-treated BPSF are shown in Fig. 3a. The content (on dry basis) of hemicellulose, acid soluble lignin, and acid insoluble lignin decreased from 22.9% to 17.9%, 1.8% to 1.6%, and 13.9% to 10.1%, respectively. After the treatment with alkali, the cellulose content of BPSF was increased from 36.9% to 41.6%. Alkali treatment dissolved a portion of the hemicellulose and lignin components as well as reduced the obstacle content (Shimizu *et al.* 2018). Similar results were reported in previous studies (Khan *et al.* 2013; Dixit and Yadav 2019). Chemical treatment destroys the complex structure of cellulose, hemicellulose, and lignin as well as increases the contact area between fiber and other materials (Dixit *et al*. 2021). Therefore, NaOH treatment of BPSF is helpful for the subsequent preparation process of composite materials and reinforcement of green applications (Dixit and Yadav 2020).

The pH variation of BPSF during the NaOH pretreatment is shown in Fig. 3b. The pH values declined with pretreatment time, likely due to the consumption of OH^-. During the NaOH pretreatment, the pH values of BPSF treated by 10 w/v %NaOH declined to 9.8 for 1.5 days. The pH variation indirectly reflects the alkali treatment process. Similar results were reported by Pei *et al.* (2014).

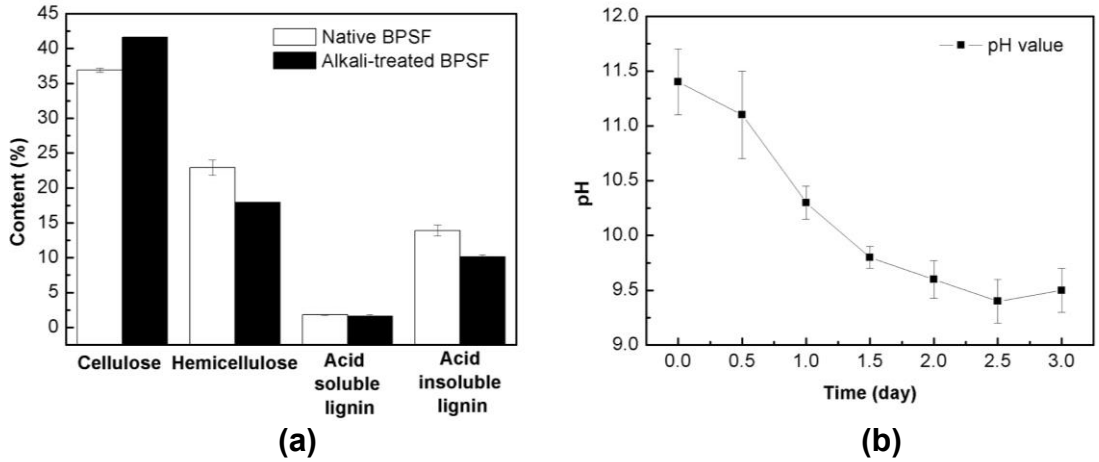

Fig. 3. Effect of alkali treatment on fiber composition and PH value of BPSF (a: effect of alkali treatment on fiber composition of BPSF; b: pH variation of samples during alkali treatment)

RSM and ANOVA Analysis for Alkali-Treated BPSF/PBAT/PLA Based Bio-Composite

Data adequacy check of the model

Table 2 lists the design and experiment results based on actual and predicted value after conducting the set of experiments provided by RSM. The resultant data were analyzed using the analysis of variance (ANOVA) to check the reliability of the mathematical model provided by RSM-BBD.

Table 2. Design and Experiment Results Based on Actual and Predicted Value using RSM

Range of Actual Variable				Actual and Predicted Value of Response			
Standard Order	Alkali-treated BPSF (g)	PBAT(g)	PLA (g)	Bending Strength (MPa)		Tensile Strength (MPa)	
				Predicted Value	Actual Value	Predicted Value	Actual Value
1	0.8	0.75	2.4	31.83	32.34	28.11	28.55
2	2.4	0.75	2.4	26.69	25.77	15.20	15.83
3	0.8	2.25	2.4	30.88	31.80	31.02	30.40
4	2.4	2.25	2.4	28.19	27.68	23.78	23.34
5	0.8	1.5	1.6	22.28	21.60	24.86	24.80
6	2.4	1.5	1.6	17.62	18.38	15.87	15.62
7	0.8	1.5	3.2	32.12	31.36	26.35	26.60
8	2.4	1.5	3.2	28.95	29.63	15.19	15.25
9	1.6	0.75	1.6	19.61	19.77	21.63	21.25
10	1.6	2.25	1.6	20.87	20.63	25.95	26.63
11	1.6	0.75	3.2	31.18	31.43	20.61	19.93
12	1.6	2.25	3.2	30.47	30.31	27.78	28.15
13	1.6	1.5	2.4	31.99	31.55	27.79	23.82
14	1.6	1.5	2.4	31.99	33.66	27.79	29.73
15	1.6	1.5	2.4	31.99	28.50	27.79	26.44
16	1.6	1.5	2.4	31.99	30.37	27.79	27.20
17	1.6	1.5	2.4	31.99	35.85	27.79	31.75

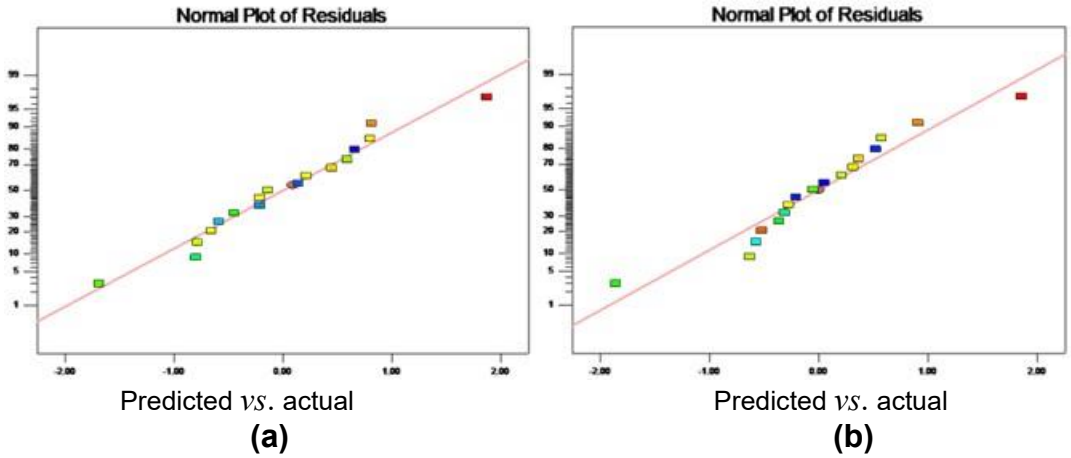

Fig. 4. Relationship between actual and predicted values of model. (a) Bending strength; (b) tensile strength

Figure 4 exhibits the predicted value provided by the RSM model and actual responses (bending strength and tensile strength) from the specific experiment. All points in the graph of predicted value *vs*. actual value were near to the diagonal line. According to Dixit *et al*. (2019), variable data points on the straight line suggests that a model is accurate. The experimentally obtained value was close to the predicted value given by design software represents the reliability of RSM.

Effect of variables on bending strength

From the data of Table 2, the following second order quadratic model was obtained using multiple regression analysis and was employed to show the role of each variable on the response value. The RSM model for the bending strength of bio-composite is shown in the following equation,

$$Y = 31.99 - 1.95x_1 + 0.14x_2 + 5.29x_3 + 0.61x_1x_2 + 0.37x_1x_3 - 0.49x_2x_3 - 1.44x_1^2 - 1.15x_2^2 - 5.30x_3^2 \quad (3)$$

where linear terms (x_1, x_2, x_3), interaction terms (x_1x_2, x_2x_3, x_1x_3), and quadratic terms (x_1^2, x_2^2, x_3^2) are listed in the mathematical equation. According to the result of ANOVA analysis, p-values less than 0.05 indicated that the corresponding coefficient terms were significant in this study (Table 3).

Table 3. ANOVA Analysis for the Bending Strength of Alkali-Treated BPSF/PBAT/PLA Composite from BBD Model

Source	Sum of Squares	df	Mean Square	F Value	p-value Prob > F	
Model	398.6584	9	44.2954	8.3535	0.0053	significant
x_1-Alkali-treated BPSF	30.5742	1	30.5742	5.7659	0.0474	
x_2-PBAT	0.1518	1	0.1518	0.0286	0.8704	
x_3-PLA	224.1196	1	224.1196	42.2658	0.0003	
x_1x_2	1.5027	1	1.5027	0.2834	0.6110	
x_1x_3	0.5505	1	0.5505	0.1038	0.7567	
x_2x_3	0.9741	1	0.9741	0.1837	0.6811	
x_1^2	8.7140	1	8.7140	1.6433	0.2407	
x_2^2	5.5620	1	5.5620	1.0489	0.3398	
x_3^2	118.4900	1	118.4900	22.3456	0.0021	
Residual	37.1184	7	5.3026			
Lack of Fit	4.4760	3	1.4920	0.1828	0.9029	not significant
Pure Error	32.6424	4	8.1606			
Cor Total	435.7767	16				
Std. Dev.	2.3027		R^2	0.9148		
Mean	28.2725		adjusted R^2	0.8053		
C.V. %	8.1448		predicted R^2	0.7186		
PRESS	122.6192		adequate precision	8.2076		

The p-value generally represents the probability of error correlated with the validation of the observed result. The F value of the quadratic model was 8.35, which represents a well-suited model for the experimental data. There was a 0.53% chance that a

"Model F-value" could occur due to noise. The reliability of the model was also confirmed by the regression correlation coefficient R^2 value at 0.91. The adequate precision value was 8.20, which indicated an adequate signal in this study. A low value for the coefficient of variation (CV = 8.14 %) demonstrated that the experiments were reliable and precise. Therefore, it can be concluded that the RSM model was suitable and appropriate to be used for predicting the final response result.

Statistical analysis showed that alkali-treated BPSF had a significant positive linear effect ($P < 0.05$) and a negative quadratic effect on bending strength. PLA had a significant positive linear effect ($P = 0.0003$) and a positive quadratic effect on bending strength. PBAT had a negative effect on bending strength. Additionally, the interaction between each two variables was observed to be insignificant. The most impactful factor was PLA ($F = 42.26$), followed by alkali-treated BPSF ($F = 5.76$).

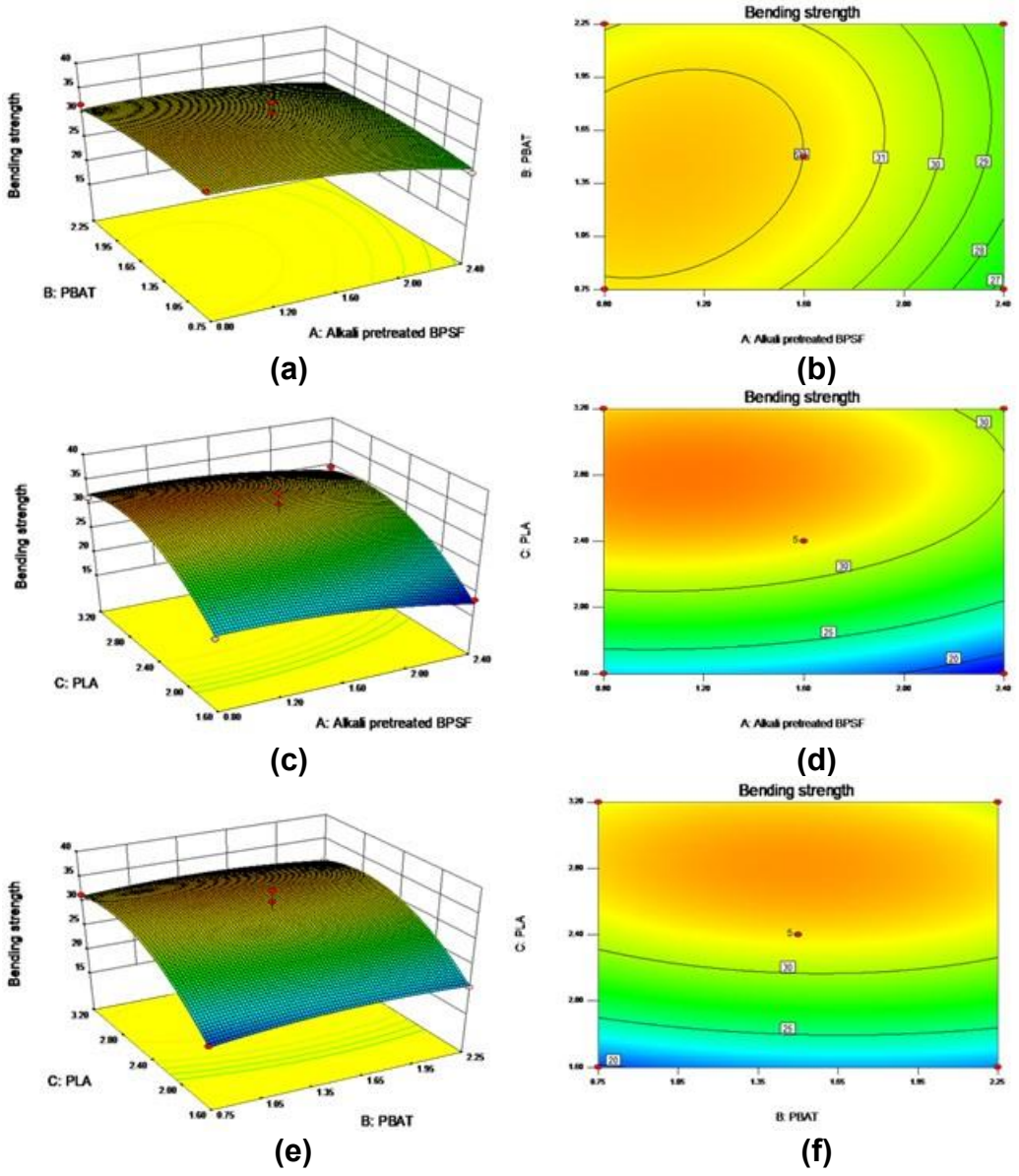

Fig. 5. Three-dimensional response surface and contour plots for the effects of two variables on the bending strength, holding the other two variables constant

Figure 5 represents the three-dimensional plots of the interactions between the dependent variables and independent variables for bending strength of bio-composite. Figures 5a and 5b show that the bending strength of bio-composite increased with decreasing the concentration of alkali treated BPSF (0.8 g to 2.4 g) when the PBAT was held at a constant level. This result signifies the remarkable effect of alkali-treated BPSF on bending strength. Figures 5c and 5d show that the bending strength increased with the increase of PLA (1.6 g to 3.2 g) when alkali-treated BPSF was kept constant. A similar trend was observed in Figs. 5e and 5f when PBAT was kept at a fixed value. The additive amount of PLA was the most impactful factor for bending strength, which was confirmed in the ANOVA analysis above. PBAT (0.75 g to 2.25 g) had an insignificant effect on bending strength of bio-composite in this experiment ($P > 0.05$), which was in agreement with the results of previous reports (Aliotta *et al*. 2020; Feng *et al*. 2020). It was reported that PBAT has good ductility and fracture elongation, whereas its mechanical properties are poor (Gao *et al*. 2021). Thus, it can be concluded that the value of bending strength is significantly affected by the addition of PLA and alkali-treated BPSF in the bio-composite. Therefore, the result above assures the considerable influence of different parameters for optimization of the bending strength of bio-composite and encourages the use of alkali-treated BPSF and PLA in the synthesis of bio-composite for packaging application.

Effect of variables on tensile strength

The statistical equation for tensile strength of bio-composite is given below.

$$Y = 27.79 - 5.04x_1 + 2.87x_2 + 0.20x_3 + 1.42x_1x_2 - 0.54x_1x_3 + 0.71x_2x_3 - 3.34x_1^2 + 0.083x_2^2 - 3.88x_3^2 \quad (4)$$

Table 4. ANOVA Analysis for the Tensile Strength of Alkali-Treated BPSF/PBAT/PLA Composite from BBD Model

Source	Sum of Squares	df	Mean Square	F Value	p-value Prob > F	
Model	397.4128	9	44.1570	7.7696	0.0066	significant
x_1-Alkali-treated BPSF	202.9788	1	202.9788	35.7147	0.0006	
x_2-PBAT	65.9705	1	65.9705	11.6077	0.0113	
x_3-PLA	0.3283	1	0.3283	0.0578	0.8170	
x_1x_2	8.0211	1	8.0211	1.4113	0.2736	
x_1x_3	1.1766	1	1.1766	0.2070	0.6629	
x_2x_3	2.0274	1	2.0274	0.3567	0.5691	
x_1^2	47.0323	1	47.0323	8.2755	0.0238	
x_2^2	0.0290	1	0.0290	0.0051	0.9450	
x_3^2	63.3792	1	63.3792	11.1518	0.0124	
Residual	39.7833	7	5.6833			
Lack of Fit	2.4993	3	0.8331	0.0894	0.9621	not significant
Pure Error	37.2841	4	9.3210			
Cor Total	437.1961	16				
Std. Dev.	2.3840		R^2	0.9090		
Mean	24.4281		adjusted R^2	0.7920		
C.V. %	9.7592		predicted R^2	0.7753		
PRESS	98.2450		adequate precision	8.6590		

The ANOVA analysis shows that p value was below 0.05, assuring the suitability of the model for tensile strength (Table 4). The Model F-value of 7.77 implies the model is significant. There is only a 0.66% chance that a "Model F-value" this large could occur due to noise. The regression correlation coefficient R^2 was 0.90, which confirmed the fitness of the model. The adequate precision value of the model was 8.65. In this analysis, the value of CV was 9.76 %. In short, the closeness of the R^2 value to 1, the adequate precision of 8.65 and the lower CV value indicated that the developed RSM model was suitable and reliable to predict the final response result

The results in Table 4 show that alkali-treated BPSF had a significant positive linear effect ($P < 0.05$) and a positive quadratic effect on tensile strength. PBAT had a significant positive linear effect ($P< 0.05$) and a negative quadratic effect on tensile strength.

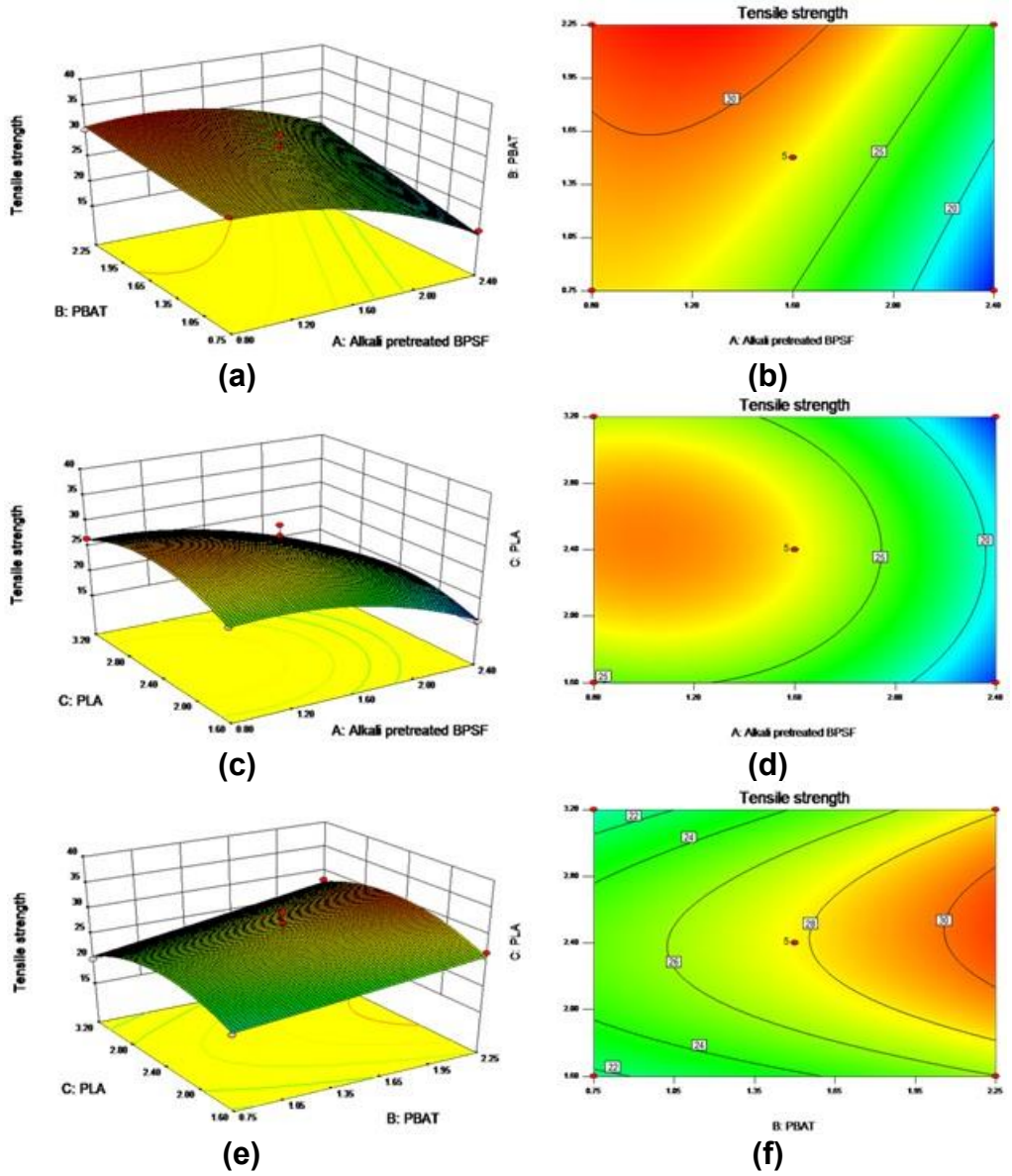

Fig. 6. Three-dimensional response surface and contour plots for the effects of two variables on the tensile strength, holding the other two variables constant

PLA had a negative linear effect (P = 0.81) and a positive quadratic effect on tensile strength. The interaction between each two variables was observed to be insignificant. The most impactful factor was alkali-treated BPSF (F = 35.71), followed by PBAT (F = 11.60).

Figure 6 shows the 3-D plots of the independent and dependent variables for tensile strength of bio-composite. The tensile strength of bio-composite continuously decreased with increasing the concentration of alkali-treated BPSF (0.8 g to 2.4 g) when the PBAT was held constantly. A similar trend was observed in Figs. 6c and 6d when the proportion of PLA remained unchanged (2.4 g). This result demonstrated that the value of tensile strength is affected in a range by the addition of alkali-treated BPSF in the bio-composite. Figures 6e and 6f show that the tensile strength of bio-composite increased with the increase of PBAT concentration (0.75 g to 2.25 g) when PLA was held constant. The additive proportion of PBAT was the most impactful factor for tensile strength, which was confirmed in the modeling results above. PLA (1.6 g to 3.2g) had an insignificant effect on tensile strength of bio-composite in this experiment (P > 0.05). Similar results were published by Aliotta *et al*. (2020) in their research article. PLA has good mechanical properties, whereas its flexibility is poor (Gao *et al.* 2021). Thus, it can be concluded from all the results above that the value of tensile strength for bio-composite is significantly affected by the addition of PBAT and alkali-treated BPSF. The tensile strength of bio-composite decreased with the addition of BPSF to some extent. The addition of PBAT can significantly improve the tensile strength of the composite.

Optimization of the RSM-BBD model

In order to check the predicted responses provided by RSM-BBD, the optimized experiment was carried out with optimum concentration of three variables. The optimum concentration of alkali-treated BPSF, PBAT, and PLA were 1.15 g, 2.09 g and 2.66 g, respectively. The predicted outputs were 32.71 MPa for bending strength and 31.19 MPa for tensile strength. The experimental results for bending strength and tensile strength of optimized composites were 32.62 MPa and 30.91 MPa (Table 5). Only small percentages of error were found in all output responses, which demonstrated the reliability of RSM-BBD statistical method (Dixit *et al*. 2021).

Characterization of the Optimized Alkali-Treated BPSF/PBAT/PLA Based Bio-Composite

The synthesized PBAT/PLA, native BPSF/PBAT/PLA and optimized alkali-treated BPSF/PBAT/PLA based composites were further characterized by using FTIR, thermogravimetry, SEM, mechanical test, contact angle test and water absorption test.

FTIR

Figure 7 shows the FTIR spectra for all prepared composites. The absorbance peak at 3309 cm^{-1} corresponds to the telescopic vibration peak of hydroxyl group (-OH), which mainly comes from the cellulose, hemicellulose, and lignin of straw fibers (Feng *et al.* 2020; Inseemeesak *et al.* 2022). The peaks near 2947 cm^{-1} (in the range of 3000 to 2850 cm^{-1}) are absorption peaks of C-H, which could be found in lignocellulosic components of BPSF, PLA, and PBAT (Feng *et al*. 2020). The peak at 1712 cm^{-1} (1750 to 1700 cm^{-1}) represents the stretching vibration peak of carbonyl (C=O) which mainly comes from hemicellulose, grease on the fiber surface, PLA, and PBAT (Correa-Pacheco *et al.* 2020; Feng *et al*. 2020). The characteristic absorption peak for aromatic ether (Ar-O) near 1266 cm^{-1} could be found in lignin (Correa-Pacheco *et al.* 2020). The stretching vibration peak

of aliphatic ether (Al-O) and aromatic ether (R-O) at 1156 and 1042 cm^{-1} could be found in BPSF, PLA and PBAT (Malinowski *et al*. 2020). The peak at 725 cm^{-1} stands for the bending vibration of -OH, which could be found in components of straw fibers (Inseemeesak *et al.* 2022).

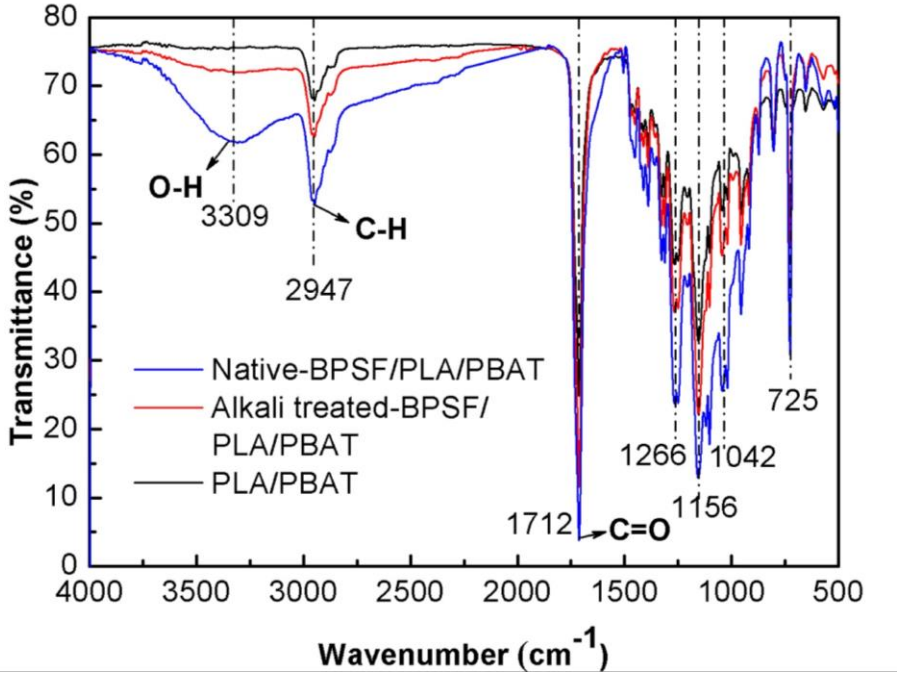

Fig. 7. FTIR of polymeric composites

The characteristic peak (3309 cm^{-1}) was not observed in PBAT/PLA. For native BPSF/PBAT/PLA and alkali-treated BPSF/ PBAT/PLA composites, the intensity of the 3309 cm^{-1} peak decreased after the alkali treatment of BPSF. A probable reason for this result was that alkali treatment destroyed the hydroxyl groups in the lignocellulosic components of BPSF as well as dissolved a portion of hemicellulose and lignin in straw fiber (Feng *et al*. 2020; Zhu *et al.* 2020; Dixit *et al*. 2021; Manral and Bajpai 2021). This result corresponded to the composition analysis of BPSF before and after alkali treatment (Fig. 3). The absorbance intensity of C-H at 2947 cm^{-1} for alkali-treated BPSF/ PBAT/PLA was lower than native BPSF/PBAT/PLA. Probable reason was that alkali treatment can destroy part of the structure of fiber components. There was no obvious change in the intensity at 1712 cm^{-1}. The absorbance intensity of carbonyl groups for alkali-treated BPSF/PBAT/PLA was slightly lower than native BPSF/PBAT/PLA. The decreasing intensity at the 1712 cm^{-1} region could attributed to the reduction of the oily layer on fiber surface and hemicellulose that was washed away by alkali treatment (Feng *et al*. 2020). The intensity for alkali-treated BPSF/PBAT/PLA at 1266 cm^{-1} significantly declined compared with native BPSF-based composite, which was contributed to the decreasing of lignin content in BPSF after alkali treatment (correspond to results in Fig. 3). The intensity of peaks near 1156, 1042, and 725 cm^{-1} decreased in varying degrees for alkali-treated BPSF/PBAT/PLA compared with native BPSF-based composites.

Results showed that alkali treatment is a key factor that could remove a portion of biomass components such as lignin and hemicellulose as well as destroy part of the structure of straw fiber (Inseemeesak *et al.* 2022). This results in increasing the contact

area and accessibility of BPSF in PBAT/PLA polymer matrix (Shimizu *et al*. 2018). Thus, the bonding ability and adhesion of fibers in composite could be improved (Zhu *et al*. 2020; Manral and Bajpai 2021).

Thermogravimetry

The TG/DTG curves for synthesized PBAT/PLA, native BPSF/PBAT/PLA and optimized alkali-treated BPSF/PBAT/PLA based composites were analyzed (Fig. 8).

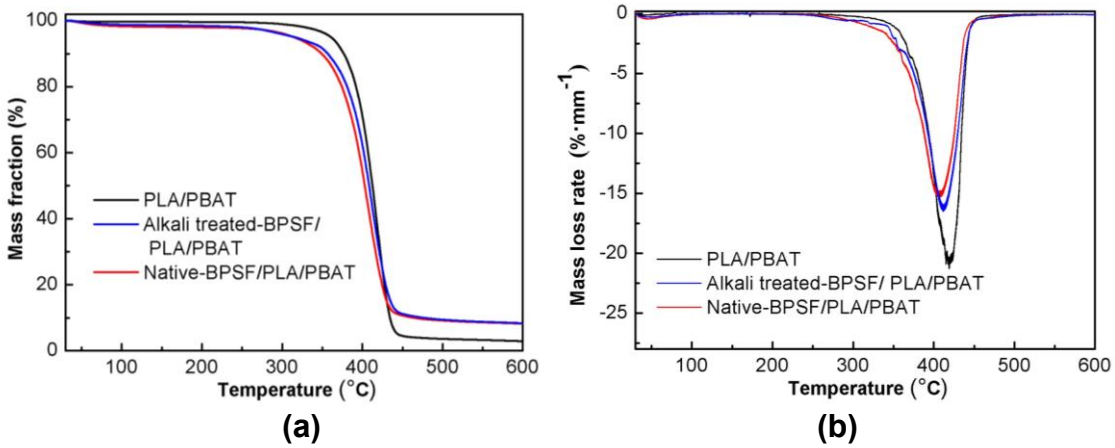

Fig. 8. TG/DTG of polymeric composites (a: TG; b: DTG)

The thermal degradation for three polymeric composites can be divided into three parts, which reveals the presence of different kinds of materials decomposed at different temperatures. From 100 to 250 °C, there was a slight decline in mass (1-3%), which mainly was caused by the evaporation of moisture trapped within the natural fiber (Rajeshkumar *et al*. 2021). All curves exhibited an extremely fast decline between 250 and 440 °C. Significant degradation started at around 318 °C for PBAT/PLA, 279 °C for alkali-treated BPSF/ PBAT/PLA, and 263 °C for native BPSF/PBAT/PLA. The second step of degradation corresponds to the decomposition of hemicellulose and cellulose presented in the BPSF as well as the degradation of PLA and PBAT matrix. Generally, the pyrolysis temperature of PLA (260 to 400 °C) and PBAT (310 to 420 °C) is higher than the main components in natural fiber. Cellulose (180 to 240 °C), hemicellulose (230 to 310 °C), and lignin (300 to 400 °C) in fiber are decomposed in sequence (Aliotta *et al*. 2020; Feng *et al*. 2020). The second stage ends at around 444 °C for PBAT/PLA, 436 °C for alkali-treated BPSF/ PBAT/PLA, and 429 °C for native BPSF/PBAT/PLA. When the temperature rose to around 440 °C, the third stage started. The mass fraction gradually tended to be stable at this stage. The third part of degradation is mainly attributed to the decomposition of lignin and other non-cellulosic molecules presented in natural fibers as well as further carbonize of pyrolysis residues from PLA and PBAT. The amount of residual for PBAT/PLA composites was 2.90%, while that of alkali-treated BPSF/ PBAT/PLA and native BPSF/PBAT/PLA were 8.22% and 8.38%, separately.

It could be concluded that the thermal stability of alkali-treated BPSF/PBAT/PLA composite was slightly higher compared with native BPSF/PBAT/PLA in terms of initial thermal degradation temperature (279 °C), pyrolysis speed (Fig. 8b), and pyrolysis residue (8.22%). This result was probably due to the uniform distribution of treated biomass in polymeric matrix (Dixit *et al*. 2021). Alkali treatment could enhance the blending

characteristics of BPSF in the polymer matrix by removing undesirable materials such as lignin and hemicellulose in crop straw. Its outcomes in better adhesion between the alkali-treated BPSF and polymer matrix. A similar outcome was published by Dixit *et al.* (2021).

SEM analysis

SEM analysis was performed to elucidate the surface morphology of PBAT/PLA, native BPSF/PBAT/PLA, and alkali-treated BPSF/ PBAT/PLA based composites. In order to examine the adhesion of treated biomass and polymer, 500 x magnification SEM images have been photographed in this test.

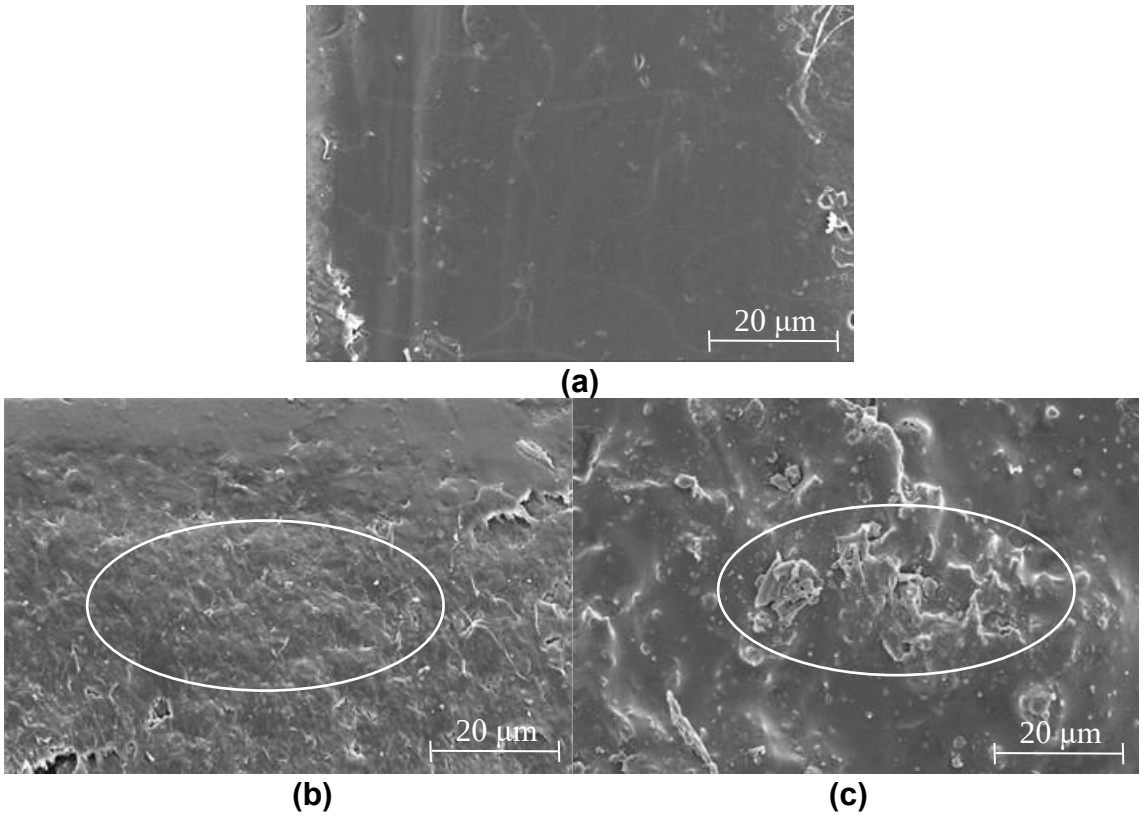

Fig. 9. SEM analysis of polymeric composites (a: PBAT/PLA, 500X; b: alkali-treated BPSF/ PBAT/PLA, 500X; c: native BPSF/PBAT/PLA, 500X)

Figure 9a exhibits the plain surface of a PBAT/PLA based composite. Uniform distribution of alkali-treated BPSF in the matrix is observed in Fig. 9b. The fractured SEM image of native BPSF/PBAT/PLA composite is observed in Fig. 9c. The surface behavior of alkali-treated BPSF-based polymer composites (Fig. 9b) shows the existence of strong biomass-polymer matrix adhesion which is similar to the plain surface of Fig. 9a. After alkali treatment, the surface roughness of bio-composite decreased as compared with native BPSF based composite (Fig. 9c). Dixit and Yadav (2019) used alkali modified wheat straw for reinforcement of polyethylene/polypropylene-based composites and observed similar result. Possible explanation for this result is that alkali treatment opened the bond between cellulose, hemicellulose, and lignin of straw fibers, thus weakened the complex lignocellulosic structure and allowed easier access of polymers (Dixit *et al.* 2021; Manral and Bajpai 2021). Additionally, alkali-treated BPSF is strongly encapsulated in PBAT/PLA matrix during hot pressing (Zhu *et al.* 2020). Stronger adhesion and enhanced

compatibility of composite materials were correlated with higher mechanical strength, which is confirmed by the mechanical test result below (Table 5).

Mechanical test

In this paper, the bending strength, tensile strength and impact strength of PBAT/PLA, native BPSF/PBAT/PLA, and alkali-treated BPSF/PBAT/PLA based composites has been investigated (Table 5).

The bending strength values of PBAT/PLA, native BPSF/PBAT/PLA, and alkali-treated BPSF/ PBAT/PLA based composites were 40.77, 27.07, and 32.62 MPa, respectively. A notable decline for bending strength was observed for polymer incorporated with native BPSF. This result signifies that the adhesion between polymer and native BPSF was poor. The bending strength increased from 27.07 to 32.62 MPa (20.50% increase) for polymer blended with native BPSF and alkali-treated BPSF, which is similar to the result published by Dixit and Yadav (2020). The tensile strength values of PBAT/PLA, native BPSF/PBAT/PLA, and alkali-treated BPSF/ PBAT/PLA based composites were 45.45, 26.53, and 30.91 MPa, respectively. A clear decrease in tensile strength was observed in polymer incorporated with untreated BPSF biomass. Moreover, the tensile strength increased from 26.53 to 30.91 MPa (16.51% increase) after the blending of alkali-treated BPSF with the polymer matrix composites. A similar result was published by Estefanía *et al.* (2018). The impact strength of PBAT/PLA, native BPSF/PBAT/PLA, and alkali-treated BPSF/PBAT/PLA based composites were 6.80, 5.51, and 6.12 kJ/m^2, respectively. Compared with native BPSF based composite, the impact strength increased slightly (11.07%) after incorporate alkali-treated BPSF with the polymer matrix. Manral and Bajpai (2021) prepared different lignocellulosic waste-based packaging material and reported a similar result in their article.

Better mechanical properties (bending strength, tensile strength, and impact strength) were observed for alkali-treated BPSF/PBAT/PLA compared with native BPSF/PBAT/PLA. The mechanical property discussed in this paper was relatively higher than other existing reports on producing sustainable bio-composites (Feng *et al*. 2020; Rajeshkumar *et al.* 2021). This result suggests the promising use of alkali-treated BPSF in a polymer matrix as well as exhibits the suitability of polymeric composites for green reinforcement packaging application.

Contact angle test

Contact angle was used to investigate the hydrophobicity of composites. The contact angle results for PBAT/PLA, native BPSF/PBAT/PLA, and alkali-treated BPSF/PBAT/PLA based composites were comparable and less than 90° (Table 5). Results shows that the contact angle for alkali-treated BPSF/ PBAT/PLA was higher than native BPSF/PBAT/PLA, which indicates that alkali treatment of BPSF enhances the hydrophobic nature of bio-composite to some extent. The difference of contact angle may be related to the surface roughness and the presence of hydrophilic groups on composite surfaces (Dixit *et al*. 2021). Alkali treatment might affect the hydrophilic groups and the surface structure of BPSF, thus enhancing the hydrophobicity of composite materials (Dixit and Yadav 2019). This result encourages the use of alkali-treated BPSF incorporated with polymer to produce polymeric composites in packaging application.

Water absorption test

The water absorption properties for composites are listed in Table 5. The water absorption result for PBAT/PLA, native BPSF/PBAT/PLA, and alkali-treated BPSF/PBAT/PLA based composites were 0.32%, 5.53%, and 4.16%, respectively. The water absorption property for native BPSF/PBAT/PLA composite was higher than other polymeric composites. This result was likely due to the unsuitable blending of biomass in a polymer matrix which was confirmed by SEM result. After the alkali treatment of BPSF, the water absorption property for bio-composite decreased, which shows better compatibility of treated biomass in polymer matrix and restricting the penetration of water. Similar phenomena were reported in published articles (Estefanía *et al*. 2018; Wang *et al*. 2018). In summary, alkali-treated BPSF, PBAT, and PLA can be potentially used as a substitute for producing polymer composite.

Table 5. Bending Strength, Tensile Strength, Impact Strength, Contact Angle, and Water Absorption Result of Polymeric Composites

Composite Material	Bending Strength (MPa)	Tensile Strength (MPa)	Impact Strength (kJ/m^2)	Contact Angle (°)	Water Absorption (%)
PBAT/PLA	40.77±1.74	45.45±2.53	6.80±0.27	86±4	0.32±0.01%
native BPSF/PBAT/PLA	27.07±2.15	26.53±0.92	5.51±0.16	67±3	5.53±0.21%
Alkali-treated BPSF/ PBAT/PLA	32.62±1.12	30.91±1.74	6.12±0.19	74±5	4.16±0.17%

CONCLUSIONS

1. Response surface methodology with a Box-Behnken experimental design (RSM-BBD) was successfully used to synthesize the optimized bio-composite based on alkali-treated banana pseudo-stem fiber (BPSF), poly-butylene adipate-co-terephthalate (PBAT), and poly(lactic acid) (PLA). The optimum concentrations were 1.15 g of alkali-treated BPSF, 2.09 g of PBAT, and 2.66 g of PLA, giving 32.62 MPa bending strength and 30.91 MPa tensile strength. The optimum results predicted by RSM-BBD were equable with the experimental results, which shows the accuracy of the model.
2. The optimized bio-composite was also characterized with the use of FTIR, thermogravimetry, SEM, mechanical test, contact angle test, and water absorption test. FTIR analysis showed that alkali treatment removed a portion of biomass components such as lignin and hemicellulose as well as destroyed part of the structure of straw fiber. The thermal stability of alkali-treated BPSF/PBAT/PLA was slightly higher than native BPSF/PBAT/PLA. SEM analysis showed that the surface roughness of alkali-treated BPSF/PBAT/PLA decreased compared with native BPSF based composite. Alkali treatment could improve the adhesion and compatibility of BPSF in the polymer matrix.
3. Alkali treatment successfully increased the bending strength, tensile strength and impact strength of bio-composite, which were 20.50%, 16.51%, and 11.07% higher than native BPSF/PBAT/PLA, respectively. Results for contact angle increased by 10.45%, whereas the water absorption decreased by 1.37% for alkali-treated BPSF/PBAT/PLA compared with native BPSF based composite. These outcomes were

associated with the use of treated-BPSF for better mechanical strength and lower hygroscopicity. Alkali-treated banana pseudo-stem fiber (BPSF) incorporated with degradable polymer could be considered as a potential substrate to synthesis bio-composite for packaging application.

ACKNOWLEDGMENTS

This research was funded by the Science and Technology Department of Hunan Province, Natural Science Foundation of Hunan Province (Grant No. 2019JJ50678) and the Scientific Research Project of Education Department of Hunan Province (Grant No. 17C0110).

REFERENCES CITED

Alarcón, L. C., and Marzocchi, V. A. (2015). "Evaluation for paper ability to pseudo stem of banana tree," *Procedia Materials Science* 8, 814 -823. DOI: 10.1016/j.mspro.2015.04.140

Albooyeh, A., Soleymani, P., and Taghipoor, H. (2022). "Evaluation of the mechanical properties of hydroxyapatite-silica aerogel/epoxy nanocomposites: Optimizing by response surface approach," *Journal of the Mechanical Behavior of Biomedical Materials* 136, 1-17. DOI: 10.1016/j.jmbbm.2022.105513

Aliotta, L., Gigante, V., Acucella, O., Signori, F., and Lazzeri, A. (2020). "Thermal, mechanical and micromechanical analysis of PLA/PBAT/POE-g-GMA extruded ternary blends," *Frontiers in Materials* 7, 1-14. DOI: 10.3389/fmats.2020.00130

Bajracharya, M. R., Manalo, A., Karunasena, W., and Lau, K.-t. (2016). "Characterisation of recycled mixed plastic solid wastes: Coupon and full-scale investigation," *Waste Management*, 72-80. DOI: 10.1016/j.wasman.2015.11.017

Bartos, A., Nagy, K., Anggono, J., Antoni, Purwaningsih, H., Mocz´o, J., and Pukanszky, B. (2021). "Biobased PLA/sugarcane bagasse fiber composites: Effect of fiber characteristics and interfacial adhesion on properties," *Composites Part A*, 1-7. DOI: 10.1016/j.compositesa.2021.106273

Cai, R. J., Wen, W., Wang, K., Peng, Y., Ahzi, S., and Chinesta, F. (2022). "Tailoring interfacial properties of 3D-printed continuous natural fiber reinforced polypropylene composites through parameter optimization using machine learning methods," *Materials Today Communications* 32, 1-11. DOI: 10.1016/j.mtcomm.2022.103985

Correa-Pacheco, Z. N., Black-Solís, J. D., Ortega-Gudio, P., Sabino-Gutiérrez, M. A., Benítez-Jiménez, J. J., Barajas-Cervantes, A., Bautista-Baos, S., and Hurtado-Colmenares, L. B. (2020). "Preparation and characterization of bio-based PLA/PBAT and cinnamon essential oil polymer fibers and life-cycle assessment from hydrolytic degradation," *Polymers* 12(1), 1-32. DOI: 10.3390/polym12010038

Dixit, S., Mishra, G., and Yadav, V. L. (2021). "Optimization of novel bio-composite packaging film based on alkali-treated hemp fiber/polyethylene/polypropylene using response surface methodology approach," *Polymer Bulletin* (3), 1-25. DOI: 10.1007/s00289-021-03646-5

Dixit, S., and Yadav, V. L. (2020). "Comparative study of polystyrene/chemically modified wheat straw composite for green packaging application," *Polymer Bulletin*

77(3), 1307-1326. DOI: 10.1007/s00289-019-02804-0

Dixit, S., and Yadav, V. L. (2019). "Optimization of polyethylene/polypropylene/alkali modified wheat straw composites for packaging application using RSM," *Journal of Cleaner Production* 240, 1-13. DOI: 10.1016/j.jclepro.2019.118228

El, M. A., and Vaudreuil, S. (2021). "Optimizing the mechanical properties of 3d-printed pla-graphene composite using response surface methodology," *Archives of Materials Science and Engineering* 12(1), 13-22. DOI: 10.5604/01.3001.0015.5928

Sánchez-Safont, E. L., Aldureid, A., Lagarón, J. M., Gámez-Pérez, J., and Cabedo, L. (2018). "Biocomposites of different lignocellulosic wastes for sustainable food packaging applications," *Composites Part B: Engineering* __, 215-225. DOI: 10.1016/j.compositesb.2018.03.037

Feng, J., Zhang, W., Wang, L., and He, C. (2020). "Performance comparison of four kinds of straw/PLA/PBAT wood plastic composites," *BioResources* 15(2), 2596-2604. DOI: 10.15376/biores.15.2.2596-2604

Gao, X., Xie, D., and Yang, C. (2021). "Effects of a PLA/PBAT biodegradable film mulch as a replacement of polyethylene film and their residues on crop and soil environment," *Agricultural Water Management* 255, 1-9. DOI: 10.1016/j.agwat.2021.107053

GB/T1040.2 (2022). "Plastics – Determination of tensile properties," Standardization Administration of China, Beijing, China.

GB/T 1043.1-2008 (2008). "Plastics – Determination of Charpy impact properties," Standardization Administration of China, Beijing, China.

GB/T 9341 (2008). "Plastics – Determination of flexural properties," Standardization Administration of China, Beijing, China.

Inseemeesak, B., Siripaiboon, C., Somkeattikul, K., Attasophonwattana, P., Kiatiwat, T., Punsuvon, V., and Areeprasert, C. (2022). "Biocomposite fabrication from pilot-scale steam-exploded coconut fiber and PLA/PBS with mechanical and thermal characterizations," *Journal of Cleaner Production* 379, 1-12. DOI: 10.1016/j.jclepro.2022.134517

Kandar, M. I. M., and Akil, H. M. (2016). "Application of design of experiment (DoE) for parameters optimization in compression moulding for flax reinforced biocomposites," *Procedia Chemistry* 19, 433-440. DOI: 10.1016/j.proche.2016.03.035

Khan, G. M. A., Shams, M. S. A., Kabir, M. R., Gafur, M. A., Terano, M., and Alam, M. S. (2013). "Influence of chemical treatment on the properties of banana stem fiber and banana stem fiber/coir hybrid fiber reinforced maleic anhydride grafted polypropylene/low-density polyethylene composites," *Journal of Applied Polymer Science* 128(2), 1-10. DOI: 10.1002/app.38197

Khosravani, M. R., and Reinicke, T. (2022). "Fracture studies of 3D-printed PLA-wood composite," *Procedia Structural Integrity* 37, 97-104. DOI: 10.1016/j.prostr.2022.01.064

Malinowski, R., Moraczewski, K., and Raszkowska-Kaczor, A. (2020). "Studies on the uncrosslinked fraction of PLA/PBAT blends modified by electron radiation," *Materials* 13(5), 1-16. DOI: 10.3390/ma13051068

Manral, A., and Bajpai, P. K. (2021). "Effect of chemical treatment on impact strength and dynamic thermal properties of Jute/PLA composites," *Materials Today: Proceedings* 34, 546-549. DOI: 10.1016/j.matpr.2020.03.110

Mansor, M. R. (2018). "Recent advances in polyethylene-based bio composites," *Natural*

Fibre Reinforced Vinyl Ester and Vinyl Polymer Composites, 71-96. DOI: 10.1016/B978-0-08-102160-6.00003-2

Murariu, M., and Dubois, P. (2016). "PLA composites: From production to properties," *Advanced Drug Delivery Reviews* 107(12), 17-46. DOI: 10.1016/j.addr.2016.04.003

Neher, B., Hossain, R., Fatima, K., Gafur, M. A., Hossain, M. A., and Ahmed, F. (2020). "Study of the physical, mechanical and thermal properties of banana fiber reinforced HDPE composites," *Materials Sciences and Applications*, 245-262. DOI: 10.4236/msa.2020.114017

Othman, S., Tarmiti, N., Shapi'i, R., Zahiruddin, S., Tawakkal, I., and Basha, R. (2020). "Starch/banana pseudostem biocomposite films for potential food packaging applications," *BioResources* 15(2), 3984-3998. DOI: 10.15376/biores.15.2.3984-3998

Pan, S., Chi, Y., Zhou, L., Li, Z., Du, L., and Wei, Y. (2020). "Evaluation of squeezing pretreatment for improving methane production from fresh banana pseudo-stems," *Waste Management* 102(2), 900-908. DOI: 10.1016/j.wasman.2019.12.011

Pei, P., Zhang, C., Li, J., Chang, S., Li, S., Wang, J., Zhao, M., Li, J., Yu, M., and Chen, X. (2014). "Optimization of NaOH pretreatment for enhancement of biogas production of banana pseudo-stem fiber using response surface methodology," *BioResources* 9(3), 5073-5087. DOI: 10.15376/biores.9.3.5073-5087

Ponni, P., Subramanian, K. S., Janavi, G. J., and Subramanian, J. (2020). "Synthesis of nano-film from nanofibrillated cellulose of banana pseudostem (*Musa* spp.) to extend the shelf life of tomato," *BioResources* 15(2), 2882-2905. DOI: 10.15376/biores.15.2.2882-2905

Rajeshkumar, G., Seshadri, S. A., Devnani, G. L., Sanjay, M. R., Siengchin, S., Maran, J. P., Al-Dhabi, N. A., Karuppiah, P., Mariadhas, V. A., Sivarajasekarf, N., and Anuf, A. R. (2021). "Environment friendly, renewable and sustainable poly lactic acid (PLA) based natural fiber reinforced composites – A comprehensive review," *Journal of Cleaner Production* 310, 1-26. DOI: 10.1016/j.jclepro.2021.127483

Ramle, S., Ahmad, N. A., Rawi, N., Zahidan, N. S., and Geng, B. J. (2020). "Physical properties and soil degradation of PLA/PBAT blends film reinforced with bamboo cellulose," *IOP Conference Series Earth and Environmental Science* 596, article no. 012021, 1-7. DOI: 10.1088/1755-1315/596/1/012021

Razaka, Z., Sulonga, A. B., Muhamada, N., Haron, C. H. C., Radzia, M. K. F. M., Ismaila, N. F., Tholibona, D., and Tharazia, I. (2019). "Effects of thermal cycling on physical and tensile properties of injection moulded kenaf/carbon nanotubes/ polypropylene hybrid composites," *Composites Part B*, 159-165. DOI: 10.1016/j.compositesb.2018.12.031

Ribeiro, G., Vanoli, S. M., Alice, M. M., Rocha, F. S., Marin, M. L., Tarcísio, L. J., Guimarães, J. M., and Henrique, D. G. (2022). "Bio-based films/nanopapers from lignocellulosic wastes for production of added-value micro-/nanomaterials," *Environmental Science and Pollution Research* 29, 8665-8683. DOI: 10.1007/s11356-021-16203-4

Shimizu, F. L., Monteiro, P. Q., Ghiraldi, P. H. C., Melati, R. B., Pagnocca, F. C., Souza, W. D., Sant'Anna, C., and Brienzo, M. (2018). "Acid, alkali and peroxide pretreatments increase the cellulose accessibility and glucose yield of banana pseudostem," *Industrial Crops and Products* 115, 62-68. DOI: 10.1016/j.indcrop.2018.02.024

Sluiter, A., Hames, B., Ruiz, R., Scarlata, C., Sluiter, J., Templeton, D., and Crocker, D. (2008). *Determination of Structural Carbohydrates and Lignin in Biomass*, Laboratory Analytical Procedure, National Renewable Energy Laboratory, Golden, CO, USA.

Tharazi, Sulong, A. B., Muhamad, N., Haron, C. H. C., Tholibon, D., Ismail, N. F., Radzi, M. K. F. M., and Razak, Z. (2017). "Optimization of hot press parameters on tensile strength for unidirectional long kenaf fiber reinforced polylactic-acid composite," *Procedia Engineering* 184, 478-485. DOI: 10.1016/j.proeng.2017.04.150

Wang, Z., Zhang, X., Xu, C., Jin, X., Nie, S., and Zhang, J. (2018). "Study on mechanical properties and water absorption of polylactic acid/wheat straw fiber composite," *Zhongguo Suliao (China plastic)* 32(8), 46-51. DOI: 10.19491/j.issn.1001-9278.2018.08.008

Xu, Z., Yang, L., Ni, Q., Ruan, F., and Wang, H. (2019). "Fabrication of high-performance green hemp/polylactic acid fibre composites," *Journal of Engineered Fibers and Fabrics* 14, 1-9. DOI: 10.1177/1558925019834497

Zegaoui, A., Derradji, M., Ma, R. K., Cai, W. A., Medjahed, A., Liu, W. B., Dayo, A. Q., Wang, J., and Wang, G. X. (2018). "Influence of fiber volume fractions on the performances of alkali modified hemp fibers reinforced cyanate ester/benzoxazine blend composites," *Materials Chemistry and Physics* 213, 146-156. DOI: 10.1016/j.matchemphys.2018.04.012s

Zhu, Z., Hao, M., and Zhang, N. (2020). "Influence of contents of chemical compositions on the mechanical property of sisal fibers and sisal fibers reinforced PLA composites," *Journal of Natural Fibers*, 101-112. DOI: 10.1080/15440478.2018.1469452

Article submitted: September 4, 2022; Peer review completed: October 1, 2022; Revised version received and accepted: October 27, 2022; Published: November 2, 2022.
DOI: 10.15376/biores.18.1.39-59